Cobalt-Boride: an Efficient and Robust Electrocatalyst for Hydrogen Evolution Reaction

SurajGupta[a], NaineshPatel[a,b,*], Antonio Miotello[b], Dushyant C. Kothari[a]

[a]Department of Physics and National Centre for Nanosciences& Nanotechnology, University of Mumbai, Vidyanagari, Santacruz (E), Mumbai 400098, India

[b]Dipartimento di Fisica, UniversitàdegliStudi di Trento, I-38123 Povo (Trento), Italy.

* Corresponding Author: **Nainesh Patel**
Lab IdEA, Department of Physics,
Università degli Studi di Trento,
Via Sommarive 14, I-38123,
Povo (Trento) – ITALY,
E-mail address: patel@science.unitn.it
Tel no: +39-0461 28 2012
Fax No.: +39-0461 28 1696

ABSTRACT: This work presents Cobalt-Boride (Co-B) as a non-noble, efficient and robust electrocatalyst for Hydrogen Evolution Reaction (HER) active in aqueous solution of wide pH values. In neutral solution, amorphous Co-B nanoparticles (30-50 nm size) generate high current density (10 mA/cm^2) at low overpotential (250 mV) with Tafel slope of 75 mV/dec following Volmer-Heyrovsky reaction mechanism. Highly active Co surface sites created by

electronic transfer from B to Co (as inferred from XPS analysis and supported by theoretical calculation) are responsible for this significant HER activity in wide range of pH (4-9) values. Stability and reusability tests also demonstrate the robust nature of the catalyst.

Keywords: Cobalt-Boride, Electrocatalyst, Hydrogen Evolution Reaction, water splitting.

Introduction:

The hydrogen based economy seems viable only when environmental and energy issues related to hydrogen production are solved by utilizing water as a H_2 source and solar energy to split water. Although water splitting by photocatalysis seems to be a promising process, it has not yet become viable because of low efficiency towards hydrogen production. Among the indirect routes, the electrochemical water splitting powered by photovoltaics is very attractive and feasible if cheaper and efficient electrocatalysts are available. Materials based on Pt metal show remarkable efficiency and stability, but are expensive and contribute in increasing the cost of an electrolyzer. Therefore, extensive research is oriented towards replacing Pt with earth-abundant materials exhibiting comparable performance for hydrogen evolution reaction (HER).

In the past decade, most of the advances [1-19] were focused on Mo-based and Ni-based alloys as possible replacement of noble metals for HER where the former systems were restricted to acidic media and latter to basic media. Recently, there have been numerous reports on Co-based catalyst [20-27] where Co-P has turned out to be an excellent electrocatalyst under acidic conditions [20-23]. Cobalt-chalcogenides [24,25]have also been reported for their superior electrocatalytic activity in acidic medium. However, these catalysts are not tested in neutral water conditions.Following the work reported by Cobo et al. [26] on Janus cobalt-based catalyst for H_2 production from neutral water electrolysis, the current interest is now deviated towards alloying d-block transition elements with metalloids (P, S, and B). Among the low cost alternatives [26-34], Co-S film [27]and Co-P/CC [28] have

exhibited the best HER activity with lowest overpotential and highest exchange current density (only one (?) order of magnitude lower than Pt) in neutral water. These advances prompted us to test other metalloid like B. Very recently molybdenum boride [4] was found active in both acidic and basic conditions.

Motivated by these reports and also on our past experience in replacing noble metal catalyst for H_2 production by hydrolysis of chemical-hydrides [35,36],we undertook the experiments on using Cobalt-Boride (Co-B) as electrocatalyst for HER and, to the best of our knowledge, results are presented for the first time. Outstanding activity was recorded with Co-B catalyst in wide range of pH values. Electronic transfer between Co and B possibly favors charge conduction during water reduction along with high resistance against deactivation and provides robustness to the catalyst.

Experimental methods:

Co-B nanoparticles were synthesized by chemical reduction method. Aqueous sodium borohydride (0.3 M), used as a reducing agent, was added to an aqueous solution of cobalt chloride (0.05 M) under continuous stirring. As bubble generation ceased, the black precipitate in the solution was filtered andextensively washed with double distilled water and ethanol to remove any traces of unreacted and unwanted ions. The black powder obtained after cleaning was dried in vacuum at room temperature. Co metal sheet specimen (2 cm x 2 cm, 1 mm thick) was also used for the sake of comparison. Prior to their use, Co sheet and Pt rod electrode was cleaned with double distilled water followed by ultra-sonication in acetone bath for 10 minutes. Co-B powder catalyst was pressed in a conventional hydraulic press at 7 tons of pressure to obtain disc-shaped pellets of diameter 18 mm and thickness 1 mm.

$HClO_4$ (0.1 M) was used as the electrolyte for all the electrochemical measurements at pH 1. For neutral pH (7)0.5 M potassium phosphate buffer solution was prepared by mixing K_2HPO_4 and KH_2PO_4 in appropriate concentrations. 0.5 M KH_2PO_4 and 0.4 M K_2HPO_4

solutions were used as electrolytes for the measurements at pH = 4.4 and pH = 9.2 respectively. All the electrochemical measurements were carried out in a 3 electrode based flat electrochemical cell (Princeton) equipped with a Pt mesh as the counter electrode. The cell was designed such that it exposes 1 cm^2 circular area of the catalyst to the electrolyte solution. Catalysts in the form of pellets were used as the working electrode. A saturated calomel electrode (SCE) (Equiptronics) with a standard potential of 0.241 V was used as the reference electrode. All the potentials measured with respect to SCE were later converted to reversible hydrogen electrode (RHE) potential by adding a value of 0.241 + (0.05916 x pH). All solutions were continuously stirred to avoid any bubble accumulation over the electrodes. The electrochemical measurements and analysis were performed using a potentiostat-galvanostat system from Autolab (PGSTAT 30) and their GPES software. Current-interrupt method was used to determine the ohmic resistance which was later compensated by subtracting iR (?) from the obtained potential values for all the measurements. Linear polarization curves were recorded in the cathodic potential range starting from -0.5 V (vs RHE) with a scan rate of 10 mV/s. Tafel slope and exchange current density values were obtained by linear fitting the plot of log (i) versus overpotential (η) in the range of η = 100-300 mV. Turnover frequency (TOF) value was determined using the procedure and equation reported by Popczun et al. [11]. BET technique was used to establish the actual surface area of the pellets used for the electrochemical measurements. Long-term stability was examined in potentiostatic mode by maintaining the potential at certain value and measuring current density with respect to time in hours. Reusability behavior of the catalyst was tested by conducting cyclic voltametric sweep in a range between -0 V and -0.5 V (vs RHE) with a scan rate of 150 mV/s.

Structural characterization of all the catalyst powders was performed by conventional X-Ray Diffractometer (XRD) using the Cu Kα radiation (λ = 1.5414 Å) in Bragg-Brentano

(θ-2θ) configuration. X-ray photoelectron spectroscopy (XPS) was used to determine the surface electronic states and the related atomic composition of the catalysts. XPS was acquired using a Kratos AXIS Ultra instrument equipped with a monochromatic Al Kα (1486.6 eV) X-ray source and a hemispherical analyzer. Electrical charge compensation was required to perform the XPS analysis. The molar ratio of elements was estimated by considering the area under the peak of the correspondent XPS spectrum. A Shirley background was subtracted from each spectrum and peaks were fitted by Voigt functions. The BET surface area of the powder catalysts was determined by nitrogen absorption at 77 K (Micromeritics ASAP 2010) after degassing at temperature of 423 K for 2 hrs.The size of Co-B NPs was examined using a transmission electron microscope (TEM). HR–TEM image and selected area electrondiffraction (SAED) pattern were recorded by JEOL-JEM 2100F TEMmicroscope operating at an accelerating voltage of 200 kV.The surface morphology of the catalyst samples was also analyzed by scanning electron microscope (SEM-FEG, JSM 7001F, JEOL) equipped with energy-dispersive spectroscopy analysis (EDS, INCA PentaFET-x3) to determine the composition of the samples.

Results and Discussion:

SEM (Fig. 1a) and bright field TEM image (Fig. 1b) of Co-B catalyst shows particle-like morphology with spherical shape and size in the range of 30-50 nm. Elemental mapping with EDS (Fig. S1) did not display any phase separation of Co and B hence suggesting that both the elements in the catalyst are well mixed at macroscopic level.. The amorphous nature of the powders with long range disorder and short range order was confirmed through XRD pattern (Fig. 1c) and HRTEM image (Fig. 1d) and which is also verified from the SAED pattern (inset of Fig. 1d). The broad peak centered at 45^{o} in XRD pattern (Fig. 1c) is assigned to the amorphous state of Co-B phase [37]. Investigation of chemical states of each elements

in catalyst by XPS (Fig. 1e and 1f) shows the presence of two peaks in Co2p level with binding energy at 778.2 and 781.6 eV with a satellite peak at 785 eV indicating that Co metal exists in both elemental and oxidized state [$Co(OH)_2$] (Fig. 1e). Similar states were also detected in B1s level with peaks at binding energies of 188.2 and 192.1 eV respectively (Fig. 1f). Most importantly, when compared to binding energy of pure B (187.1 eV), the elemental B in the catalyst is positively shifted by 1.1 eV suggesting an electron transfer from alloying B to vacant d-orbital of metallic Co making former electron deficient while later enriched with electron as indicated by small negative shift (0.2 eV) in the Co elemental peak. These results suggest that the surface of Co-B catalyst is composed of electron enriched Co sites bonded with B and cobalt hydroxide [$Co(OH)_2$] in ratio of 1:1.38 as obtained from peak area. Similar oxides species are also noticed by Sun et al. (Co-S catalyst) [27] and Cobo et al. (Janus cobalt catalyst) [26]. The electronic transfer from B to Co allows B to act as the sacrificial agent in order to partially protect Co from oxidation. The surface elemental atomic ratio of Co/B is 1.61, signifying that mixed composition of Co-B with oxidized cobalt, mainly $Co(OH)_2$, ispresent on the surface.

To clarify the electron interaction between Co and B, first principles study of charge transfer in Co-B alloy in their crystalline and amorphous forms was performed using $Dmol^3$ module [38] of material study~~io~~ within density functional theory. For the cystalline form, CoB and Co_2B are considered in orthorhombic (space group Pbnm) and tetragonal (spacegroup I4/mcm) structures respectively, while for amorphous we have considered 14 and 22 atoms clusters for CoB and Co_2B, respectively. From the Mulliken's charge transfer analysis, electrons are transferred from Co atom to B atom for both CoBand Co_2B in crystalline form which shows high electronegativity of B atom in Co-B alloys. On the other side, in the case of Co-B amorphous clusters, reverse electron transfer is observed from B to Co atom making Co more electronegative in disordered Co-B arrangement.Since in the

present case the synthesized Co-B alloy is in completely amorphous state thus the above theoretical result confirms the experimental finding through XPS on electron transfer. These Co atom sitesenriched with electron are highly active for catalytic reaction,as also suggested in case of hydrogenation [39,40] and hydrolysis reactions [35, 36]. Recently Carenco et al. [41] distinguish the electron transfer in transition metal (Co, Ni, and Fe) boride where electron transfer occurs from Mto B in boron-rich systems (MB_x, $x \geq 2$) and from B to M formetal-rich borides (MB_x, $x \leq 2$).This finding of electronically enriched metal was also confirmed on the bases of magnetic and Mössbauer measurements and metal binding energy shifts observed byX-ray photoelectron spectroscopy [42, 43]. In all cases the metal-boride was in amorphous state. However, most of the first principle calculations [44,45]show that the totalelectron transfer should occur from metal to boron in relationwith relative electronegativities but here the building of Co-B was considered to be well ordered and crystalline.

The catalyst powder was cold-pressed in the form of pellets and employed as working electrode in a typical three-electrode electrochemical cell. Water with neutral pH will be used in future to produce H_2 for fuel-cell on the household level, therefore the synthesized catalysts were tested first in potassium phosphate buffer solution with pH 7. The linear polarization curves of Co-B catalyst along with that of Co and Pt metal are presented in Fig. 2. The HER activity achieved by Co-B is significantly higher than that obtained with Co metal and the onset overpotential observed (vs RHE), was as low as -70 mV (at 0.5 mA/cm^2). Beyond this value, rapid rise in the cathodic current was induced at further negative potentials. The overpotential (η) of only -178 mV and -251 mV was required to attain moderate current density of 2 mA/cm^2 and 10 mA/cm^2, respectively, where substantial H_2 evolution occurs (Table S2).While these current densities were noted at -50 mV and -176 mV using Pt metal as working electrode. The overpotential required to achieve these current

densities is considerably higher for almost all reported earth abundant element-based molecular and solid-state catalysts such as Janus cobalt catalyst [26],Cu_2MoS_4 [46],CoP_4N_2[32] and NiWS [17] catalyst at neutral pH (see supporting information for comparison of various catalysts in Table S3). The exception is only the Co-S [27] and Co-P/CC [28] catalyst which displayed a lower overpotential than that of Co-B.

The linear fitting of Tafel plot (inset of Fig. 2) gives the Tafel slope of 75 mV/dec and exchange current density (J_o) of 0.25 mA/cm^2 for Co-B nanocatalyst. On the other hand, unfavorable values of these parameters were observed for Co metal (7.0 x 10^{-4} mA/cm^2 and 133 mV/dec) (Table S1 of supporting information). Amongst the non-noble electrocatalysts studied so far, the highest J_o reported is for the present Co-B catalyst and for Co-S catalyst [27]. The enrichment of d-band electron density, on Co sites of the Co-B catalyst, improves the electron-donating ability to enhance its HER catalytic activity and therefore generate high current densities at lower overpotentials than that obtained by Co metal. Similar characteristic was reported for Ni-Mo-N_x alloy [13] where the presence of N modifies the d-band electron density of Ni-Mo alloy to favor reaction kinetics.

The Tafel slope is comparable to the value reported for Co-S [27],M-MoS_3 (M=Fe, Co or Ni) [47],and Cu_2MoS_4[46] HER catalyst at pH 7, but this value is nowhere near to the standard values for HER reaction steps that are: 120, 40, and 30 mV/dec for Volmer, Heyrovsky, and Tafel mechanism respectively. Thus, here it is difficult to establish the reaction mechanism; but the value of 75 mV/dec may suggest the Volmer-Heyrovsky route for HER [4,22,27,46,47]. The value of Tafel slope which is considerably lower than that of Volmer step (~120 mV/dec) hints that the process of H^+ ions adsorption is not the rate-limiting step. This adsorption process is conceivable because of the presence of electron enriched Co sites on the catalyst surface which can easily assist to reduce H_2O and adsorb H according to the Volmer step ($H^+ + e^- \rightarrow H_{ads}$). On the other hand, after the coverage of these

Co active sites by H_{ads}, unavailability of electron hinders the desorption of H_2 molecule by Heyrovsky step ($H_{ads} + H^+ + e^- \rightarrow H_2$). HER activity per site of a catalyst is investigated by evaluating turnover frequency (TOF) using BET surface area (16.5 m^2/g) of Co-B catalyst (procedure reported in Supporting Information). At η=250 mV for exchange current density of 10 mA/cm^2, TOF was calculated to be 0.086 s^{-1} (Table S3). This value is underestimated because the actual active Co sites on the surface (containing also boron) are not known. The TOF value is higher than that reported for Co-S (0.017 s^{-1})[27] and Janus Cobalt (0.022 s^{-1})[26] at neutralpH.

The HER catalyst should be active and stable in any reaction medium even though the neutral medium is preferable for environmental purpose. Thus, the HER activity of Co-B catalyst was investigated in aqueous solutions of different pH values, namely: 1, 4.4and 9.2. These values are selected on bases that sea water and rain water are the main sources of water which are relatively more basic (pH 8-9.5) and acidic (pH 4.2-6) in nature respectively.For extreme pH value strong acid was used while phosphate buffer solution was tuned to establish the remaining pH values. As observed in linear polarization curves, Co-B catalyst displayed extremely high HER activity for all pH values in contrast to Co metal (Fig. 3a, 3b,and 3c). The plot (Fig. 3d) of overpotential (at 2 mA/cm^2) and exchange current density values as a function of pH shows that pH 9.2 is the most favorable medium for Co-B catalyst (table S1). Lowering the pH of the solution leads to the decrease in HER activity with lowest electrochemical parameters recorded in acidic medium (pH 1 and pH 4.4).The values of J_o = 5 x 10^{-2} mA/cm^2 and η = 216 mV at 2 mA/cm^2 in acidic solution are comparable to Ni and Mo based non-noble HER catalysts including Ni_2P [11], Mo_2C/CNT [10], MoN [13], MoB [4], and Mo_2C [4]. Water electrolysis in acidic medium proceeds by the formation of hydronium ions (H_3O^+) which later discharge on the catalyst surface for adsorption of H [1]. Higher Tafel slopes of 108 and 102 mV/dec in low pH (4.4 and 1 respectively) solutions

indicate that the Volmer step for adsorption of H ion is the rate limiting step, which explains the poor adsorption of H_3O^+ ions in the acidic media, by the Co active sites. At higher pH (9.2), on the other hand, neutral water molecules are easily reduced on the Co active sites by hydrogen adsorption while OH^- ions provide the necessary ion-conduction in the solution to deliver high current density at low overpotential. These results indicate that Co-B electrocatalyst is highly active in wide pH range: a rare property exhibited by the HER electrocatalysts.

Furthermore, the stability of Co-B catalyst was investigated by measuring the current density under constant overpotential vs RHE as a function of time (Fig. 4a). Under neutral pH, the current density varies by small value in 44 hours while maintaining overpotential of 250 mV. Thus, over that time period, a linear build-up of charge is registered. Durability test conducted on pH values of 9.2 and 4.4 (Fig. S2 of supporting information) demonstrated similar charge accumulation over the long period of time (44 hours). To test the ability to withstand industrial workload, Co-B catalyst was cycled 1000 times in the potential range between 0 to -0.5 V vs RHE at pH 7 in phosphate buffer (Fig. 4b). After 1000 cycles, HER activity of Co-B catalyst remained unchanged (or changed marginally) for pH values of 9.2 and 4.4 (Fig. S3), except in highly acidic medium. Under pH 1, after 10 cycles, the visible dissolution of Co-B powder was monitored. Nevertheless, these results illustrate the robust nature of the Co-B catalyst under wide range (pH 4-9) of environmental conditions.

Conclusion:

In summary, we introduced Co-B amorphous nanoparticles (30-50 nm size), synthesized by facile method, as possible substitute of noble metal based electrocatalyst for HER. In water with neutral pH, an overpotential of only -251 mV was required to attain a current density of 10 mA/cm^2. The present overpotential, with related current density, is considerably lower than almost all the previously reported results of the earth abundant element-based molecular

and solid-state catalysts, with favorable values of Tafel slope of 75 mV/dec, and exchange current density of 0.25 mA/cm^2 at neutral pH. Highly active Co surface sites, created by electronic transfer from B to Co, are responsible for the remarkable HER activity and robust nature in wide range of pH (4-9) values. Under neutral pH, the current density varies by small value during 44 hours test while maintaining overpotential of 250 mV: this proves the stability of the Co-B catalyst. Finally, after 1000 cycles, the HER activity of Co-B at pH 7 remained unchanged.

Acknowledgment

We acknowledge L. Calliari for XPS analysis and N. Bazzanella for SEM analysis. The research activity is partially supported by UGC-UPE Green Technology Project, India and PAT (Provincia Autonoma di Trento) project ENAM in cooperation with Istituto PCB of CNR (Italy).

References

[1] Y. Li, H. Wang, L. Xie, Y. Liang, G. Hong, H. Dai, J. Am. Chem. Soc. 133 (2011) 7296–7299.

[2] A.B. Laursen, S. Kegnæs, S. Dahl, I. Chorkendorff, Energy Environ. Sci. 5 (2012) 5577–5591.

[3] M.A. Lukowski, A.S. Daniel, F. Meng, A. Forticaux, L. Li, S. Jin, J. Am. Chem. Soc. 135 (2013) 10274−10277.

[4] H. Vrubel, X. Hu, Angew. Chem. Int. Ed. 51 (2012) 12703 –12706.

[5] Y. Yu, S. Huang, Y. Li, S. Steinmann, W. Yang, L. Cao, Nano Lett. 14 (2014) 553–558.

[6] Z. Wu, B. Fang,Z. Wang, C. Wang, Z. Liu,F. Liu, W. Wang, A. Alfantazi, D. Wang, D. P. Wilkinson, ACSCatal.3 (2013) 2101−2107.

[7] Z. Chen, D. Cummins, B. N. Reinecke, E. Clark, M. K. Sunkara, T. F. Jaramillo, Nano Lett. 11 (2011) 4168-4175.

[8] D. J. Li, U. N. Maiti, J. Lim, D. S. Choi, W. J. Lee, Y. Oh, G. Y. Lee, S. O. Kim, Nano Lett. 3 (2014) 1228-1233.

[9] L. Liao, S. Wang,J. Xiao, X. Bian, Y. Zhang, M. D. Scanlon, X. Hu, Y. Tang, B. Liu, H. H. Girault, Energy Environ. Sci. 7 (2014) 387-392.

[10] W.F. Chen, C.H. Wang, K. Sasaki,N.Marinkovic, W. Xu, J. T. Muckerman, Y. Zhu, R. R Adzic, Energy Environ. Sci. 6 (2013) 943–951.

[11] E.J. Popczun, J.R. McKone, C.G. Read, A.J. Biacchi, A.M. Wiltrout, N. S. Lewis, R.E. Schaak, J. Am. Chem. Soc. 135 (2013) 9267−9270.

[12] D. Voiry, H. Yamaguchi, J. Li, R. Silva, D. C. B. Alves, T. Fujita, M. Chen, T. Asefa, V.B. Shenoy, G. Eda, M. Chhowalla, Nature Mater. 12 (2013) 850–855.

[13] ZonghuaPu, Qian Liu, Abdullah M. Asiri, Abdullah Y. Obaid, Xuping Sun, J. of Power Sources 263 (2014) 181-185.

[14] J.R. McKone, B.F. Sadtler, C.A. Werlang, N.S. Lewis, H.B. Gray, ACSCatal.3 (2013) 166−169.

[15] J.R. McKone, E.L. Warren, M.J. Bierman, S.W. Boettcher, B.S. Brunschwig, N.S. Lewis, H.B. Gray, Energy Environ. Sci. 4 (2011) 3573–3583.

[16] S. Martinez, M. Metikos-Hukovic, L. Valek, J. Mol. Catal. A: Chem. 245 (2006) 114–121.

[17] P.D. Tran,S.Y.Chiam, P.P. Boix, Y. Ren, S.S. Pramana, J. Fize, V. Artero, J. Barber, Energy Environ. Sci. 6 (2013) 2452–2459.

[18] N.S. Alhajri, H. Yoshida, D. H. Anjum, A. T. Garcia-Esparza,J. Kubota, K. Domen, K. Takanabe, J. Mater. Chem. A 1 (2013) 12606-12616.

[19] W. F. Chen, J. T. Muckerman, E. Fujita, Chem. Comm. 49 (2013) 8896-8909.

[20] P. Jiang,Q. Liu, C Ge,W. Cui,ZPu,A.M Asiri,X. Sun, J. Mater. Chem. A 2 (2014) 14634-14640.

[21] E.J. Popczun,C.G. Read,C.W. Roske,N.S. Lewis,R.E. Schaak,Angew. Chem. Int. Ed. 53 (2014)5427 –5430.

[22] Q. Liu, J. Tian,W. Cui, P. Jiang,N. Cheng,A.M. Asiri,X. Sun, Angew. Chem. Int. Ed. 53 (2014) 6710 –6714.

[23] H. Du,Q. Liu, N. Cheng; A.M. Asiri,X. Sun,C.M. Li, J. Mater. Chem. A 2 (2014) 14812-14816.

[24] A.I. Carim,F.H. Saadi,M.P. Soriaga,N.S. Lewis, J. Mater. Chem. A 2 (2014) 14835-14839.

[25] M.S. Faber,R. Dziedzic,M.A. Lukowski,N.S. Kaiser,Q. Ding,S. Jin, J. Am. Chem. Soc. 136 (2014) 10053−10061.

[26] S. Cobo, J. Heidkamp, P.A. Jacques, J. Fize, V. Fourmond, L. Guetaz, B. Jousselme, V. Ivanova, H. Dau, S. Palacin, M. Fontecave, V. Artero, Nat. Mater. 11 (2012) 802-807.

[27] Y. Sun, C. Liu, D. C. Grauer, J. Yano, J. R. Long, P. Yang, C. J. Chang, J. Am. Chem. Soc. 135, (2013) 17699−17702.

(1) [28]JingqiTian, Qian Liu, Abdullah M. Asiri, Xuping Sun, J. Am. Chem. Soc.136 (21) (2014) 7587–7590.
[29] P. Du, R. Eisenberg, Energy Environ. Sci. 5 (2012) 6012-6021.

[30] B. Cao, G. M. Veith, J. C. Neuefeind, R. R. Adzic, P. G. Khalifah, J. Am. Chem. Soc. 135 (2013) 19186−19192.

[31] H. Lei, A. Han, F. Li, M. Zhang, Y. Han, P. Du, W. Lai, R. Cao, Phys. Chem. Chem. Phys. 16 (2014) 1883-1893.

[32] L. Chen, M. Wang, K. Han,P. Zhang, F. Gloaguen, L. Sun, Energy Environ. Sci. 7 (2014) 329–334.

[33] L. G. Bloor, P. I. Molina, M. D. Symes, L. Cronin, J. Am. Chem. Soc. 136 (2014) 3304−3311.

[34] D. Kong, H. Wang, Z. Lu, Y. Cui, J. Am. Chem. Soc. 136 (2014) 4897-4900.

[35] N. Patel, A. Miotello, V. Bello, Appl. Catal. B: Environ. 103 (2011) 31–38.

[36] N. Patel, R. Fernandes, G. Guella, A. Kale, A. Miotello, B. Patton, C. Zanchetta, J. Phys. Chem. C. 112 (2008) 6968-76.

[37] Y.D. Wang, X.P. Ai, Y.L. Cao, H.X. Yang, Electrochem.Commun. 6 (2004) 780–784.

[38] B. Delley, J. Chem. Phys. 92 (1990) 508–513.

[39] H. Li, X. Chen, M. Wang, Y.Xu,Appl.Catal. A: Gen. 225 (2002) 117–130.

[40] H. Li, Y. Wu, H. Luo, M. Wang, Y. Xu, J. Catal. 214 (2003) 15–25.

[41] S. Carenco, D. Portehault, C. Boissiere, N. Mezailles, C. Sanchez, Chem. Rev. 113 (2013) 7981–8065.

[42] J. D. Cooper, T. C. Gibb, N. N. Greenwood, R. V. Paris, Trans. Faraday Soc. 60 (1964) 2097.

[43] Y. Okamoto, Y. Nitta, T. Imanaka, S. Teranishi, J. Chem. Soc.,Faraday Trans. 75 (1979) 2027.

[44] B. Xiao, J. D. Xing, S. F. Ding, W. Su, Phys. B 403 (2008) 1723.

[45] C. T. Zhou, J. D. Xing, B. Xiao, J. Feng, X. J. Xie, Y. H. Chen, Comput. Mater. Sci. 44 (2009) 1056.

(2) [46]P. D.Tran, M.Nguyen, S. S. Pramana, A. Bhattacharjee, S. Y. Chiam, J.Fize, M. J.Field, V. Artero, L. H.Wong, J.Loo, Barber, Energy Environ. Sci. 5 (2012) 8912-8916.

(3) [47] D. Merki, H. Vrubel, L. Rovelli, S. Fierro, X. Hu, Chem. Sci. 3 (2012) 2515-2525.

Figure Caption:

Figure 1: (a) SEM image, (b) Bright field TEM image, (c) XRD pattern, (d) HRTEM image with inset showing SAED pattern; and X-ray Photoelectron Spectra of (e) $Co2p_{3/2}$ and (f) B1s level of Co-B catalyst.

Figure 2: Linear polarization curves with iR correction for Pt, Co-B, and Co in 0.5 M potassium phosphate buffer with pH 7 obtained with scan rate of 10 mV/s. Inset shows the corresponding Tafel plot for the Co-B catalyst.

Figure 3: Linear polarization curves with iR correction for Co-B catalyst compared with Co metal in (a) pH 1 (0.1 M $HClO_4$), (b) pH 4.4 (0.5 M KH_2PO_4) and (c) pH 9.2(0.4 M K_2HPO_4) obtained with scan rate of 10 mV/s. (d) Plot of overpotential (at 2 mA/cm^2) and exchange current density values as a function of pH values of the solution used to test the Co-B catalyst.

Figure 4: (a) Plot of charge build-up versus time at constant overpotential of 250 mV and (b) Recycling behavior (scan rate of 150 mV/s) for Co-B catalyst acquired in 0.5 M potassium phosphate buffer with pH 7. Inset of the plot shows the variation in current density over this long period of time.

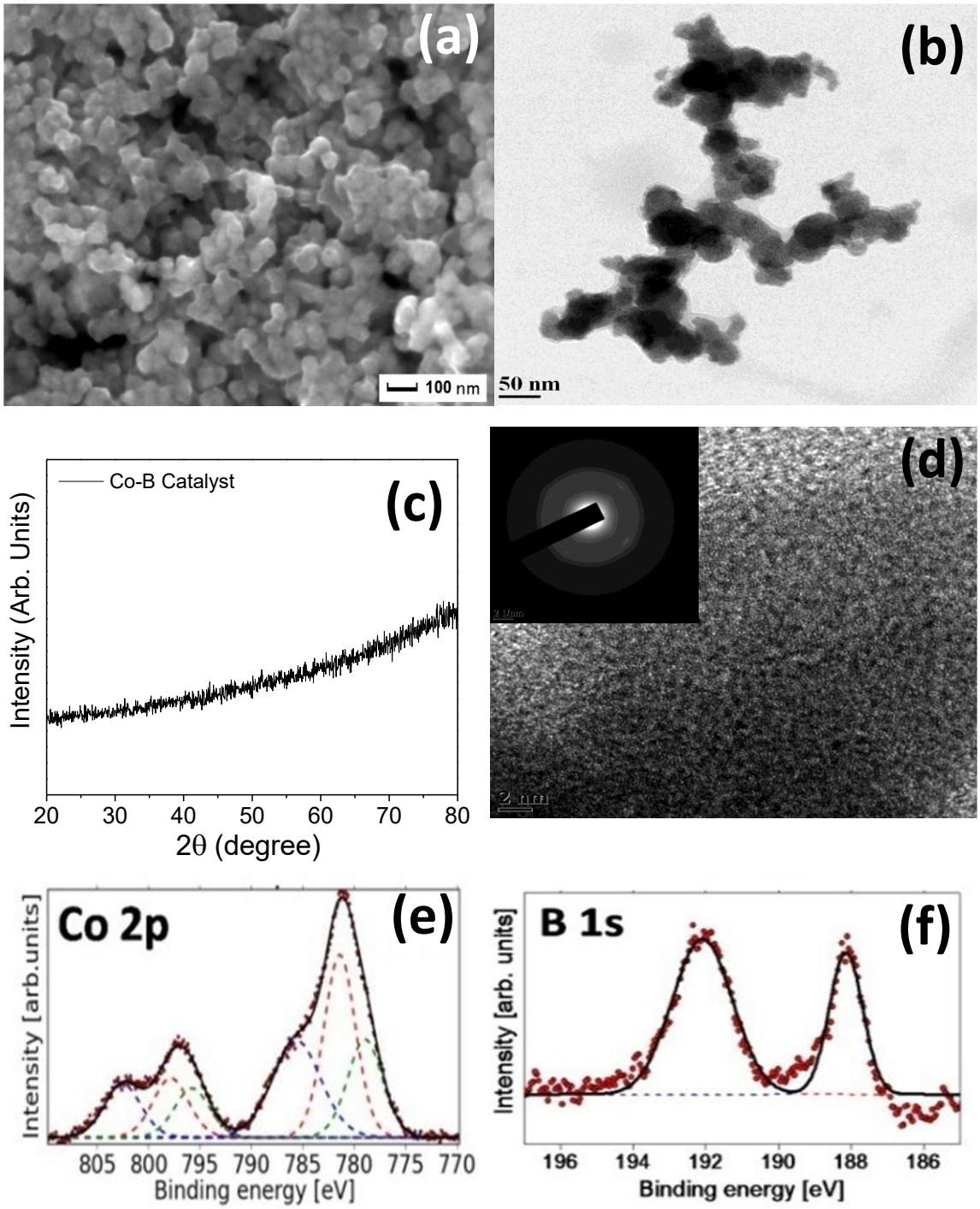
(a)
100 nm
(b)
50 nm
(c)
Co-B Catalyst
Intensity (Arb. Units)
20 30 40 50 60 70 80
2θ (degree)
(d)
2 nm
(e)
Co 2p
Intensity [arb.units]
805 800 795 790 785 780 775 770
Binding energy [eV]
(f)
B 1s
Intensity [arb. units]
196 194 192 190 188 186
Binding energy [eV]

Figure 1:

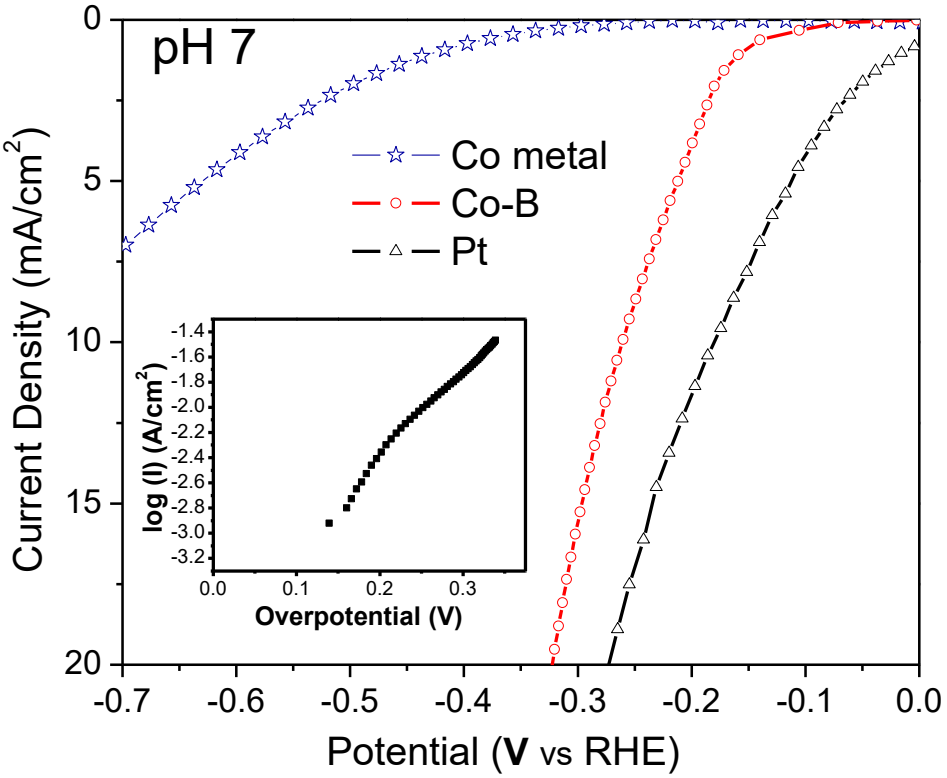
pH 7
Co metal
Co-B
Pt
Current Density (mA/cm^2)
Potential (**V** vs RHE)
log (I) (A/cm^2)
Overpotential (V)
0
5
10
15
20
-0.7
-0.6
-0.5
-0.4
-0.3
-0.2
-0.1
0.0
-1.4
-1.6
-1.8
-2.0
-2.2
-2.4
-2.6
-2.8
-3.0
-3.2
0.0
0.1
0.2
0.3

Figure 2:

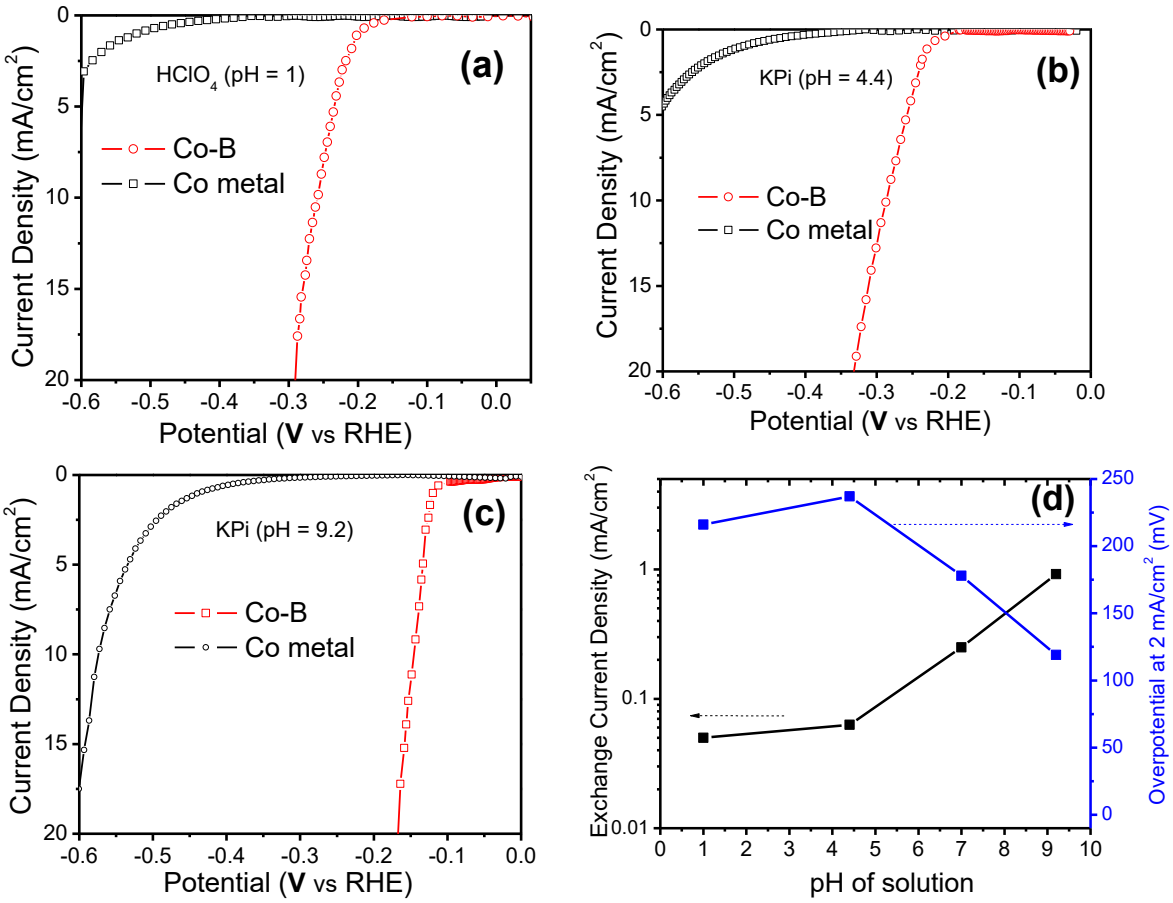
(a)
HClO4 (pH = 1)
Co-B
Co metal
Current Density (mA/cm2)
Potential (V vs RHE)
(b)
KPi (pH = 4.4)
Co-B
Co metal
Current Density (mA/cm2)
Potential (V vs RHE)
(c)
KPi (pH = 9.2)
Co-B
Co metal
Current Density (mA/cm2)
Potential (V vs RHE)
(d)
Exchange Current Density (mA/cm2)
Overpotential at 2 mA/cm2 (mV)
pH of solution

Figure 3:

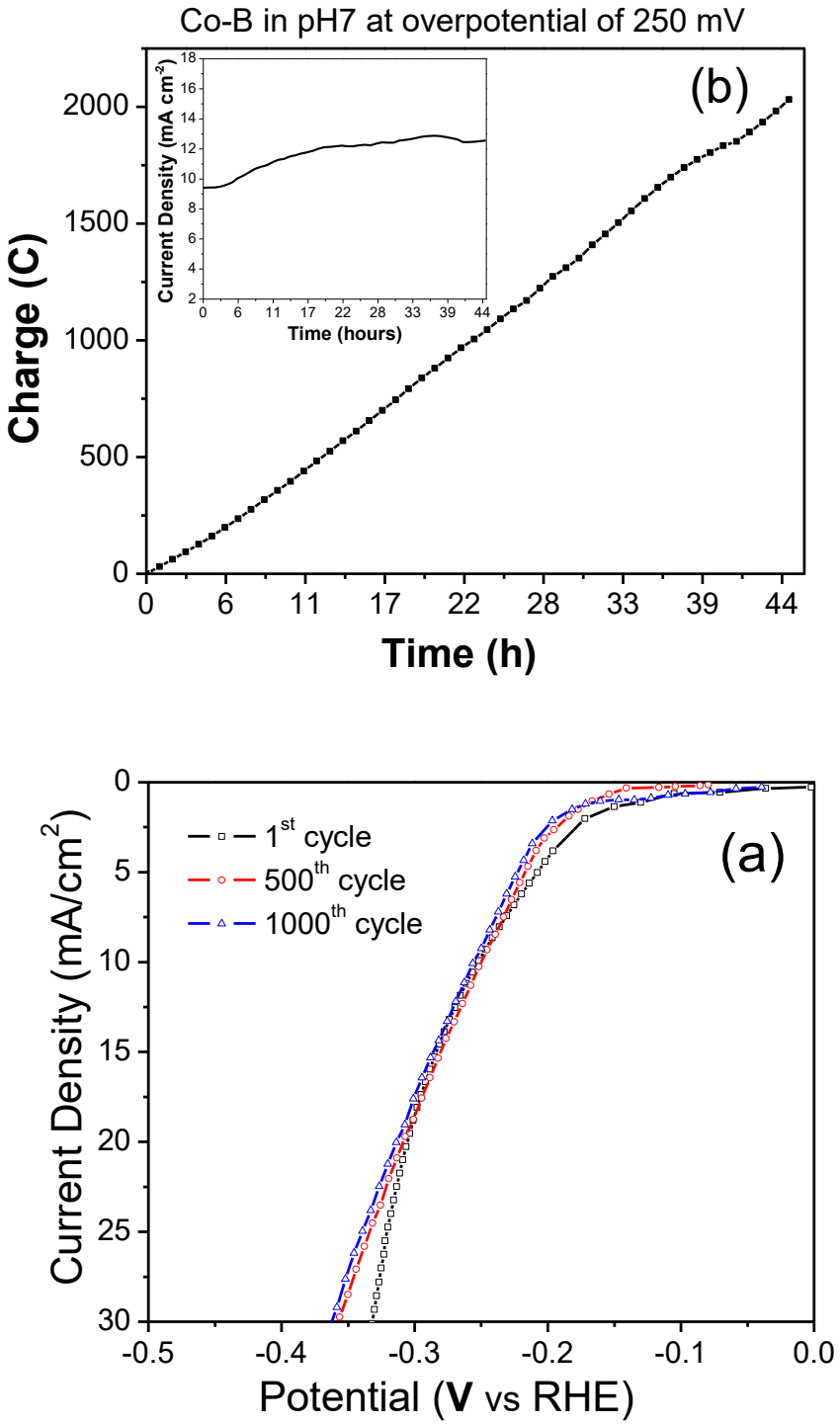
Co-B in pH7 at overpotential of 250 mV
(b)
Charge (C)
Time (h)
Current Density (mA cm-2)
Time (hours)
(a)
1st cycle
500th cycle
1000th cycle
Current Density (mA/cm2)
Potential (V vs RHE)

Figure 4: